Light Control of Growth Form in Colonial Reef Corals: Computer Simulation

Abstract. *Computer simulation with plotter output reveals the close interrelation between ambient light and the skeletal morphogenesis of the massive Caribbean reef coral* Montastrea annularis. *This technique illustrates a new quantitative approach to evaluating ecological growth responses of colonial organisms.*

Computer simulation techniques that were previously successful in geometric analyses of skeletal development of molluscan shells (*1*) have now been applied in a quantitative study of coral skeletal morphogenesis. Morphological alterations that lead to flattening of the corallum and a decrease in the skeletal accretion rate that corresponds to increased water depth have been documented among massive reef corals (*2–5*). In the Caribbean area, these alterations are found, in varying degrees of development, in *Porites astreoides* Leseur, *Meandrina meandrites* (Linnaeus), *Stephanocoenia michelinii* Milne Edwards and Haime, *Colpophyllia natans* (Müller), *C. breviserialis* Milne Edwards and Haime, *Dichocoenia stokesi* Milne Edwards and Haime, *Montastrea cavernosa* (Linnaeus), and *M. annularis* (Ellis and Solander). The best example is probably *Montastrea annularis*, which exhibits wide morphological variation over its depth range (0.3 to 80 m) (*6*). At Carrie Bow Cay, Belize, the characteristic form (Fig. 1) is approximately hemispherical in shallow water (1 to 5 m), peaked or columnar at intermediate depths (5 to 25 m), and platelike at the greatest depths of the species (> 25 m). Over the same depth interval, the maximum annual skeletal growth increment decreases from 1.1 to 0.3 cm.

Such morphological differentiation has been attributed to several causes, both genetic and environmental (*7–9*). The adaptive response of skeletal growth rate to the systematically varying direction and intensity of underwater illumination has been discussed for several reef corals, including *Montastrea annularis* (*2–5*). Biological experiments linking skeletal calcification rate to ambient light intensity (*3*, *10–12*) strongly support this explanation; however, little attempt has been made to quantitatively relate the experimental evidence to observed morphological trends on reefs. This information gap is partly a result of the difficulty of controlling the environmental variables over a sufficiently long growth interval to obtain valid results.

The use of the computer allowed us to assemble the pertinent factual information, to simulate growth according to a hypothetical model, and, by the relative success or failure of the simulation, to rapidly evaluate the accuracy of the model. Taking as the growth model the results of the biological experiments, together with underwater radiance data from the Caribbean and measured geometric growth characteristics of *Montastrea annularis*, we developed a computer program to simulate, with graphic output, the skeletal morphogenesis of this species under a variety of lighting conditions.

The specific model that we used for the response of coral skeletal growth to light is the exponential function $r = R(1 - e^{-k(I - Ic)})$, where r is the skeletal growth rate in centimeters per year, R is the maximum skeletal growth rate of the species at saturation light intensity, I is the light intensity in foot-candles (1 foot-candle = 10.76 lux), Ic is the minimum threshold light intensity below which no long-term growth takes place, and k is a constant. This function is based on similar expressions that apply to organisms growing in relation to resources that are limiting in quantity (*13*). It incorporates three concepts developed from experimental studies of coral growth in relation to light intensity: (i) the rates of processes related to calcification (for example, carbon dioxide fixation, oxygen production, and calcium uptake) and calcium carbonate deposition increase proportionately (≃ linearly) with subsaturating light intensity (*11*, *12*); (ii) there exists a saturating light intensity above which the rate of calcification does not increase (*11*); and (iii) there exists a minimum threshold light intensity below which long-term growth cannot be maintained (*5*). The minimum intensity is not strictly compensation intensity because coral growth does occur, albeit slowly, even in total darkness (*3*, *11*). However, these studies (*3*, *11*) were conducted over short time intervals, and the results may prove to be invalid if extended over time periods of months or years. The absence of hermatypic corals in shallow-water caves or in very deep water argues strongly that light of some minimum intensity is necessary for continued survival.

The exponential function was fitted by a reduced major axis line (*14*) to the light and carbon dioxide fixation curve reported by Barnes and Taylor (*11*). The minimum threshold light intensity, Ic, was set at 29 foot-candles, the vertical radiance value at the normal maximum depth (45 m) of the species (*6*). The maximum growth rate, R, was set at 1.1 cm per year, which is the maximum annual growth increment measured for any colony from Carrie Bow Cay.

Information on submarine light comes from Roos (*5*), who measured radiance distributions on Piscadera Baai reef, Curaçao, at water depths of 5, 10, and 20 m. The reported data, which represent two-dimensional radiance fields in the solar plane, are the means of light-meter readings (given in microamperes) that have been mathematically corrected for variations in solar altitude and azimuth angle (*15*). We calculated least squares regression lines for specific angular radiances with depth in order to be able to generate approximate radiance distributions for any depth down to 45 m. Also, because Roos's data were taken in open water, we added a 5 percent reflection value (*16*) to account for the bottom reflection from white carbonate substrate on which the corals grow. We checked these data on the reef at Carrie Bow Cay with a portable radiometer-photometer (*17*). Although lack of time and manpower prohibited our making a comprehensive light survey, we were able to establish that the vertical radiance attenuation is similar for the reefs at Curaçao and Belize, and that the reflection added to the Curaçao data was approximately correct.

The computer program also uses morphological information from measurements of 15 colonies of *Montastrea annularis* (including the hemisphere, column, and plate morphotypes) collected from different depths and habitats at Carrie Bow Cay and Jamaica. The variables measured include (i) maximum annual growth increment (distances between alizarin red S dye markers and between annual density growth bands shown on x-radiographs); (ii) mean distance between corallites; (iii) mean intercorallite distance prior to budding; (iv) angle and mode of budding; and (v) orientations of the corallites relative to the growth surface.

Growth in the computer program starts from a predetermined base, usually a segment of a circle. This is chosen to approximate the shape of an early growth stage of a colony. Corallites are positioned on the base at the mean intercorallite distance and are oriented perpendicular to the colony surface. Growth events are annual to facilitate ready comparison with annual density bands as seen in the x-radiographs of coral slab

sections (*4*). An event begins with a routine that determines the radiance received by each of the growing polyps. The light is converted functionally into an annual growth increment, which is added to the terminal growth position of the corallite. The new positions, when taken together, define the next annual growth surface. The corallites are then projected forward, perpendicular to the new growth surface. After the calculations, the axes of the corallites and the new growth surface are drawn by a drum plotter (California Computer Products). The above procedure is repeated for the desired number of years.

Budding of new corallites occurs as space is created by the curvature and divergence of existing corallites on the differentially expanding growth surface. New buds form either between other corallites or at the periphery of the colony. The former develop according to a space-available criterion (that is, whenever the mean intercorallite distance prior to budding is exceeded) at an angle which bifurcates the angle between flanking corallites. Peripheral buds develop laterally from the epitheca and reorient during growth in the direction of maximum radiance. Theoretically, peripheral buds can form on any colony morphotype. However, they actually occur almost exclusively on columns and plates which, because of their geometry and slow growth rate, do not rapidly increase their polypary tissue area. In the extreme case of absolutely flat plates, no tissue increase is possible without peripheral budding. Because polypary tissue increases for the life of the colony at a rate that is suggested by Goreau (*3*) to be independently regulated by food supply, we introduced a program control to guarantee minimum tissue growth, in the form of peripheral budding, for cases in which there is insufficient skeletal growth of the existing growth surface. Thus, peripheral growth occurs whenever the annual increase in tissue surface area falls below 10 percent, and new buds are added only up to the 10 percent limit. This rate corresponds to the observed rate of surface area increase of the flat plate morphotype.

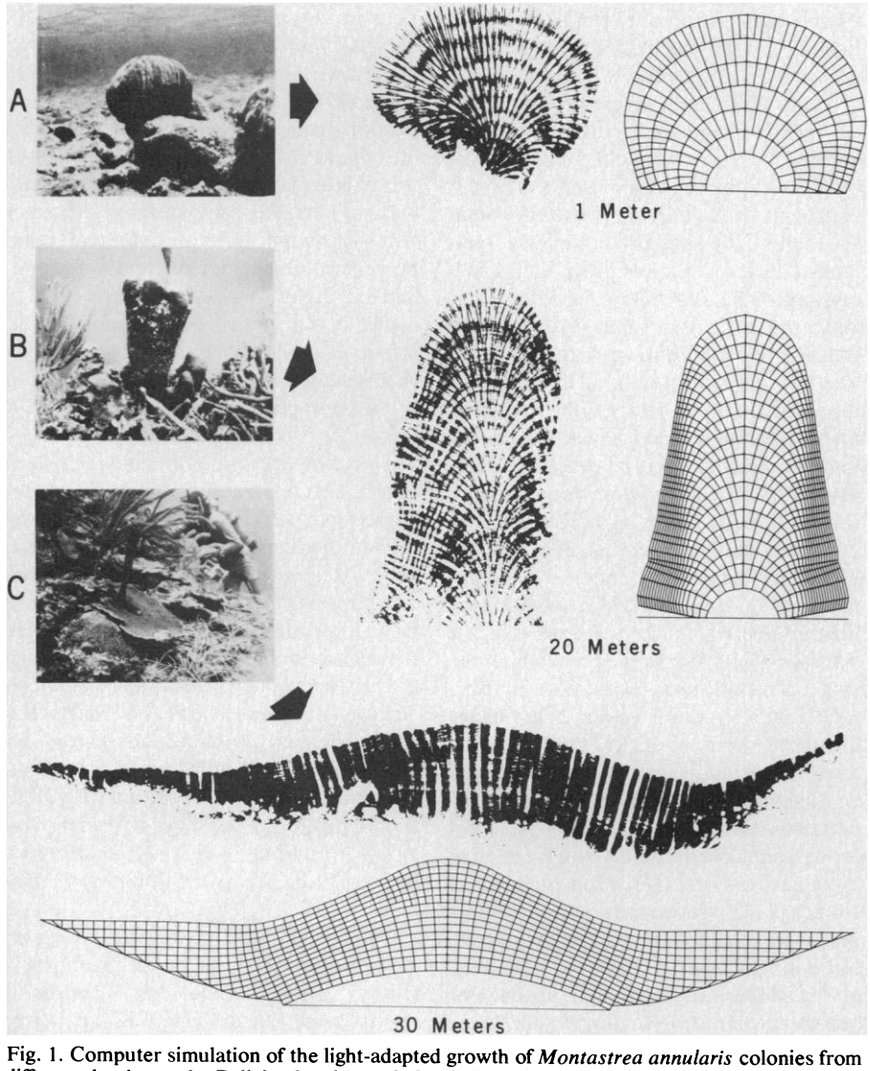

Fig. 1. Computer simulation of the light-adapted growth of *Montastrea annularis* colonies from different depths on the Belizian barrier reef (Carrie Bow Cay). Photographs show three colony morphotypes [hemisphere (A), column (B), and plate (C)] in natural habitats. Positive prints of x-radiographs, made from thin skeletal slabs cut vertically through specimens, show annual growth bands and corallite growth history. Drawings are the graphic output from a computer program that simulates colony growth patterns observed in the respective x-radiographs. The concentric lines delineate annual growth increments; the radial lines represent the axes of the corallites. Scale of x-radiographs and simulations, × ½.

Figure 1 shows results of the simulation of the light-adapted growth of three colonies of *Montastrea annularis* living at different water depths at Carrie Bow Cay. There is a close similarity between the simulated growth patterns and the real colonies as revealed in the x-radiographs, particularly with regard to the annual growth increments and their variation with vertical angle and depth, the curvature of individual corallites and their divergence and convergence with respect to each other, and the budding of new corallites. The same morphological information and program logic and controls apply for all simulations; only the nature of the light field is changed. In each case, the number of years of growth counted from the chosen reference base matches the actual specimen.

Although the growth form of *Montastrea annularis* can be influenced by symbiotic growth interaction (*9*) and platy colonies of this species can have adaptive advantages on sloping surfaces (*8*), our model of response to light, by its ability to account for the gross morphological variation, indicates that light intensity and distribution provide the major ecological control of skeletal morphogenesis. The model further indicates that genetic differences between shallow- and deep-water populations (*7*) are not required to explain these morphological trends of *Montastrea annularis*.

Variation of the morphological input parameters should permit simulation of other massive light-adapted species. Simulations of branched species could also be achieved by introducing a routine to allow for an axial as well as a diffuse mode of growth. To be most effective, however, such simulations would have to be developed in three dimensions.

The success of our model illustrates the potential application of computer simulation techniques in evaluating the growth pattern responses of colonial organisms to various other ecological parameters. For example, computer simulation could be considered in studies relat-

ing water movement to growth in branched scleractinian corals, octocorals, poriferans, and hydrozoans (*18, 19*). Computer simulation allows investigators to alter each morphological parameter independently or in combination with others, thereby permitting exploration of the exact nature and limits of the adaptive mechanisms. Computer output in the form of maps or serial sections could serve as plans for constructing physical models (*19*). Such models could then be tested experimentally in a flume with flow measuring equipment (*18*), and the results could be compared with the actual structures of corals living in known energy regimes on a reef.

RICHARD R. GRAUS
IAN G. MACINTYRE

Department of Paleobiology, National Museum of Natural History, Washington, D.C. 20560

References and Notes

1. D. M. Raup, *Proc. Natl. Acad. Sci. U.S.A.* **47**, 602 (19 → *Science* **138**, 150 (19 → *J. Paleontol.* **40**, 1178 (19 → *ibid.* **41**, 43 (1967).
2. T. F. Goreau, *Biol. Bull. (Woods Hole, Mass.)* **116**, 59 (1959); P. J. Roos, *Stud. Fauna Curaçao* **20**, 1 (1964).
3. T. F. Goreau, *Ann. N.Y. Acad. Sci.* **109**, 127 (1963).
4. I. G. Macintyre and S. V. Smith, in *Proceedings of the 2nd Coral Reef Symposium* (Great Barrier Reef Committee, Australia, 1974), vol. 2, p. 277.
5. P. J. Roos, thesis, Drukkerij Elinkwijk, Utrecht (1967).
6. T. F. Goreau and J. W. Wells, *Bull. Mar. Sci.* **17**, 443 (1967).
7. P. Dustan, thesis, State University of New York at Stony Brook (1975).
8. T. F. Goreau and W. D. Hartman, in *Mechanisms of Hard Tissue Destruction*, R. F. Sognnaes, Ed. (American Association for the Advancement of Science, Washington, D.C., 1963), p. 25.
9. ———, *Science* **151**, 343 (1966).
10. S. Kawaguti and D. Sakamoto, *Bull. Oceanogr. Inst. Taiwan* **4**, 65 (1948).
11. D. J. Barnes and D. L. Taylor, *Helgol. Wiss. Meeresunters.* **24**, 284 (1975).
12. B. E. Chalker and D. L. Taylor, *Proc. R. Soc. London Ser. B* **190**, 323 (1975).
13. R. W. Eppley and P. R. Sloan, *Physiol. Plant.* **19**, 47 (1965); T. R. Parsons, R. J. LeBrasseur, J. D. Fulton, O. D. Kennedy, *J. Exp. Mar. Biol. Ecol.* **3**, 39 (19 → J. Caperon, S. A. Cattell, G. Krasnick, *Limnol. Oceanogr.* **16**, 599 (1971).
14. J. Imbrie, *Bull. Am. Mus. Nat. Hist.* **108**, 215 (1956).
15. Mean vertical radiance values for Piscadera Baai reef, Curaçao, given by Roos (*5*, table 11), are 923 μa at 5 m, 662 μa at 10 m, and 253 μa at 20 m.
16. A. Ivanoff, N. Jerlov, T. H. Waterman, *Limnol. Oceanogr.* **6**, 105 (1961).
17. UDT-40X Opto-Meter, United Detector Technology, Santa Monica, Calif.
18. J. A. Chamberlain, Jr., and R. R. Graus, *Bull. Mar. Sci.* **25**, 112 (1975).
19. R. R. Graus, J. A. Chamberlain, Jr., A. M. Boker, *Am. Assoc. Petrol. Geol. Spec. Pap.*, in press; S. A. Wainwright and J. R. Dillon, *Biol. Bull. (Woods Hole, Mass.)* **136**, 130 (1969); R. Reidl, *Biologie der Meereshölen* (Parey, Hamburg, 1966); C. W. Stearn and R. Riding, *Lethaia* **6**, 187 (1973).
20. J. A. Chamberlain, Jr., *Palaeontology* **12**, 48 (1969).
21. Computer time and fieldwork in Belize for R.R.G. was supported by a Smithsonian postdoctoral fellowship, 1974–75. We thank G. Capone for assistance with computer graphics, B. Boykins for preparing and x-radiographing slabbed specimens, and P. Dustan, W. Oliver, J. Pierce, J. Porter, and D. Raup for reviewing the manuscript. Coral samples from Jamaica were provided by P. Dustan.

30 March 1976: revised 6 July 1976

Calcium-Independent Modulation of Cyclic GMP and Activation of Guanylate Cyclase by Nitrosamines

Abstract. *Nitrosamines markedly increase concentrations of guanosine 3′,5′-monophosphate (cyclic GMP) in several tissues from the rat and in human colonic mucosa. These agents are effective in the absence of extracellular calcium and enhance guanylate cyclase activity in tissue homogenates. Stimulation of cyclic GMP was greatest in liver, where the carcinogenic activity of nitrosamines is also most pronounced.*

There is evidence to suggest that guanosine 3′,5′-monophosphate (cyclic GMP) may promote cell growth and transformation (*1*), although not all data are consistent with this hypothesis (*2*). In the study reported here, we demonstrate that nitrosamines, compounds with well-established carcinogenic and mutagenic properties which may be formed in the digestive tract from dietary constituents and drugs (*3–5*), are potent agonists of guanylate cyclase activity in tissue homogenates and of cyclic GMP accumulation in tissue slices. The action of nitrosamines to increase cellular cyclic GMP concentrations can be fully expressed in the absence of extracellular Ca^{2+}. The Ca^{2+}-independent action of nitrosamines on cyclic GMP and their ability to activate guanylate cyclase in tissue homogenates resemble the recently described properties of sodium azide (*6–8*), but differ from those of most of the currently recognized physiologic agonists of cyclic GMP, such as cholinergic and α-adrenergic stimuli. These latter agents both require Ca^{2+} to increase cellular cyclic GMP accumulation and fail to activate guanylate cyclase in broken cell preparations (*9, 10*). With nitrosamines, enhancement of guanylate cyclase activity and cyclic GMP accumulation are greatest in liver, where their carcinogenic action is also most pronounced (*5*). The effects of *N*-methyl-*N'*-nitro-*N*-nitrosoguanidine (MNNG), a potent carcinogen with a considerable propensity toward free radical formation (*11*), are particularly striking. Indeed, MNNG may be the most potent agonist of guanylate cyclase activity yet identified.

Slices of liver, renal cortex, and lung were prepared with a Stadie-Riggs microtome, and scrapings of colonic mucosa were obtained with a glass slide. Organs were excised from 300-g male Sprague-Dawley rats fasted 18 hours and then anesthetized with pentobarbital. Human colonic mucosa was obtained from patients undergoing therapeutic segmental resections for carcinoma or diverticular disease. To assay cyclic GMP content, tissue was initially incubated for 20 minutes at 37°C in 2 ml of Krebs-Ringer bicarbonate buffer (Ca^{2+}, 1.5 m*M*) with glucose and albumin (1 mg/ml) in either the absence or presence of 2 m*M* 1-methyl-3-isobutyl-xanthine (MIX) to inhibit cyclic nucleotide breakdown. Test agents were then added and incubations continued for the times indicated. Incubations were terminated by homogenizing tissue in 5 percent trichloroacetic acid at 0° to 4°C. Cyclic GMP was then extracted and measured by radioimmunoassay, as previously reported (*12*), while the cyclic adenosine monophosphate (AMP) content of the same extracts was determined by the protein-binding method (*12*). To assay guanylate cyclase activity, tissue was gently homogenized in a solution containing 0.25*M* sucrose and 5 m*M* tris buffer, *p*H 7.4 (25 mg/ml). Appropriate dilutions of whole homogenates or the 100,000*g* soluble and particulate fractions were employed. Activity was determined from the conversion of [α-^{32}P]guanosine triphosphate (GTP) to cyclic GMP, using a reaction mixture (1 m*M* GTP, 4 m*M* Mn^{2+}, creatine phosphate–creatine phosphokinase GTP regenerating system) and a two-step chromatographic technique (AG 50 WX4 followed by neutral alumina) for purification of cyclic GMP that have been described in detail (*13*). Reactions were conducted at 37°C for 7 minutes. Cyclic GMP formation was linear with time for at least 10 minutes and with respect to added protein. Dithiothreitol (2.5 m*M*) was included in homogenates and reaction mixtures of lung and colonic mucosa to prevent "autoactivation" of the enzyme (*14*) observed in these two tissues. The MIX and MNNG were obtained from Aldrich Chemical Co., Milwaukee, Wis.; diethylnitrosamine (DEN), dibutylnitrosamine (DBN), nitrosopiperidine (NP), hydroxylamine (NH_2OH), and sodium nitrite were purchased from Fisher Scientific Co., Pittsburgh, Pa. Sources of all other reagents have been reported (*7, 12, 13, 15*). Each experiment was repeated at least twice.

As shown in Table 1, MNNG, DEN, DBN, and NP increased hepatic cyclic GMP 4- to 33-fold in 2 minutes. With MNNG, increases in hepatic cyclic GMP were detected within 15 seconds (3-fold) and levels remained elevated for at least